Steel and Composite Structures, *Vol. 20, No. 6 (2016) 1345-1368*
DOI: http://dx.doi.org/10.12989/scs.2016.20.6.1345

Probabilistic-based assessment of composite steel-concrete structures through an innovative framework

José C. Matos [*1], Isabel B. Valente [1a], Paulo J.S. Cruz [2b] and Vicente N. Moreira [1c]

[1] *ISISE, Department of Civil Engineering, School of Engineering, University of Minho, Guimarães, Portugal*
[2] *Lab2PT, School of Architecture, University of Minho, Guimarães, Portugal*

(*Received October 10, 2015, Revised January 11, 2016, Accepted February 19, 2016*)

Abstract. This paper presents the probabilistic-based assessment of composite steel-concrete structures through an innovative framework. This framework combines model identification and reliability assessment procedures. The paper starts by describing current structural assessment algorithms and the most relevant uncertainty sources. The developed model identification algorithm is then presented. During this procedure, the model parameters are automatically adjusted, so that the numerical results best fit the experimental data. Modelling and measurement errors are respectively incorporated in this algorithm. The reliability assessment procedure aims to assess the structure performance, considering randomness in model parameters. Since monitoring and characterization tests are common measures to control and acquire information about those parameters, a Bayesian inference procedure is incorporated to update the reliability assessment. The framework is then tested with a set of composite steel-concrete beams, which behavior is complex. The experimental tests, as well as the developed numerical model and the obtained results from the proposed framework, are respectively present.

Keywords: probabilistic-based assessment; uncertainty sources; model identification; reliability assessment; Bayesian inference; composite steel-concrete structures

1. Introduction

Safety assessment embraces all required measures to assess the structural performance of existing structures, particularly, its safety. In the past decades, several authors have been using probabilistic-based safety assessment procedures, showing that structures classified as unsafe according to current design standards have enough performance when assessed by probabilistic procedures (Henriques 1998, Enright and Frangopol 1999, Enevoldsen 2001, Casas and Wisniewski 2011, Caspeele and Taerwe 2014). Lately, Bayesian inference has been used to update the probabilistic models with gathered data from the assessed structure (Strauss *et al*. 2008, Bergmeister *et al*. 2009). Although most of the applications concern reinforced concrete structures, Zona *et al*. (2010) use these procedures for the safety assessment of continuous composite steel-concrete girders.

---

*Corresponding author, Ph.D., Assistant Professor, E-mail: jmatos@civil.uminho.pt
[a] Ph.D., Assistant Professor, E-mail: isabelv@civil.uminho.pt
[b] Ph.D., Full Professor, E-mail: pcruz@arquitectura.uminho.pt
[c] Ph.D. Candidate, E-mail: vicente.nmoreira@gmail.com

http://www.techno-press.org/?journal=scs&subpage=6 ISSN: 1229-9367 (Print), 1598-6233 (Online)

Two interesting studies have been also published regarding the reliability assessment of composite structures. Mujagić and Easterling (2009) presented a comprehensive study that evaluates the reliability of composite beams and proposes revised resistance factors, through the use of reliability analysis techniques with analytical strength calculation models, in which a method to consider the effect of the degree of shear connection on the strength reduction factor is proposed. Barbato *et al*. (2014) employed a methodology for probabilistic response analysis based on the First-Order Second Moment (FOSM) method, in conjunction with a response sensitivity computation through the Direct Differentiation Method (DDM), to study the variability in the nonlinear structural response of composite steel-concrete beams.

This paper presents an innovative probabilistic-based structural assessment framework, which combines, in a single algorithm, some of the structural assessment techniques mentioned above with a new procedure to identify optimal solutions, based on an evolutionary algorithm, a hybrid decision-making procedure and a Bayesian inference tool, providing the objective treatment of different sources of uncertainty (Matos 2013, Matos *et al*. 2015), see Fig. 1(a). Initially, model identification adjusts model parameters through a procedure that uses a nonlinear finite element model (NL FEM) to obtain the structure predicted performance. Then, such procedure seeks the minimum difference between observed and predicted performance in order to obtain the most likely values of material and mechanical properties, see Fig. 1(b). A convergence criterion, based on the accuracy of numerical and experimental data, is established for the optimization algorithm. In this case, an evolutionary strategies algorithm, a global optimization algorithm, is used (Beyer and Schwefel 2002). This algorithm yields a set of candidate optimal solutions from which the best model is selected based on previous knowledge, by considering the probability of each solution to occur and an engineering judgment procedure. A probabilistic model is respectively obtained by introducing randomness in model parameters, provided by model identification. Each parameter is then updated, based on collected data, through a Bayesian inference procedure. At the end, a reliability index is computed through a comparison between the resistance and effects of load curves. This index provides information about the condition state of the assessed structure. According to SAMCO report (Rücker *et al*. 2006), this framework is classified as a level 5 assessment class (model-based assessment of existing structures), once it combines probabilistic simulation methods, with a stochastic NL FEM and data from measurement of material properties and dimensions.

Although the framework can be applied to any type of structures, its applicability to composite structures has very interesting aspects related to its specific behavior and obtained failure modes. Accordingly, by applying this framework it will be possible to predict more accurately the structural response of composite structures, emphasizing its versatility and potentiality. Additionally, and although this methodology can be applied to new structures, its application aims at better characterizing existing structures for which there is limited information. Therefore, the developed framework, which addresses different sources of uncertainty, is tested and validated with a set of composite steel-concrete beams, which were loaded up to failure in laboratory. This controlled experiment is crucial since, unlike real structures, destructive tests can be extensively employed to evaluate the accuracy of the prediction.

2. Probabilistic-based structural assessment

The probabilistic-based structural assessment framework is divided in two main stages (Matos 2013, Matos *et al*. 2015), see Fig. 1(a). Firstly, model identification searches for the most likely values of model parameters based on the combination of numerical methods and experimental measurements. Within this procedure, numerical results are fitted to collected data from real structure, by adjusting model parameter values. This is attained by an optimization algorithm that minimizes the distance between both data, given by a fitness function. An evolutionary algorithm, which belongs to the global optimization algorithms, is respectively used for this purpose (Beyer and Schwefel 2002). Once the improvement in the fitness function is equal or lower than a threshold value, the optimization procedure stops. From this stage, an updated NL FEM is obtained. This model can predict, more accurately, the structural response. The reliability assessment aims to assess the structure performance, considering randomness in model parameters. Within this procedure, a distribution is initially assigned to each parameter of the updated numerical model. This distribution is then updated through a Bayesian inference procedure, with retrieved data from visual inspection, characterization tests or monitoring systems. A Latin Hypercube Sampling (LHS) method (Olsson *et al*. 2003, Shields *et al*. 2015), with an Iman and Conover (1982) algorithm integrated, is respectively used to randomly generate the correlated model parameters. A set of failure loads is obtained from the analysis of all generated NL FEMs. The resistance curve is then obtained from a distribution fitting procedure to this set. A reliability index is finally computed by relating, through a limit state function, the obtained resistance with the effects of load curve. This index can be considered as an updated performance indicator for the structure under evaluation.

The main disadvantage of such framework is its computational cost. Therefore, and in order to overcome it, a sensitivity analysis procedure is recommended. This procedure consists in measuring the fitness function variation with each input parameter, resulting in an importance measure, b_k, for each evaluated parameter (Matos 2013, Matos *et al*. 2015), expressed by Eq. (1)

$$b_k = \sum_{i=1}^{n} (\Delta y_k / y_m)/(\Delta x_{ik} / x_{im}) \cdot \mathrm{CV}[\%] \tag{1}$$

being Δy_k the variation in structural response due to a deviation of Δx_k in input parameter mean value x_m, y_m the average response, n the number of generated parameters and CV the parameter coefficient of variation. The critical parameters, i.e., those that present a higher influence on the overall structural response, are then identified through this analysis.

2.1 Model identification

According to Fig. 1(b), the first step of proposed structural assessment framework is the model identification procedure, which results in an updated deterministic numerical model. During this procedure, model parameters are automatically adjusted in order to obtain a deterministic numerical model that accurately reproduces the experimental data. The framework runs the nonlinear numerical model for each set of input parameters obtaining, from each run, the corresponding results. In parallel, experimental data is gathered. The cumulative difference between numerical and experimental data, is computed through an objective function, denominated by fitness function, f, expressed by Eq. (2)

$$f = \sum_{i=1}^{n} \left| y_i^{num} - y_i^{\exp} \right| \Big/ \max(y^{\exp}) \cdot 1/n \ [\%] \tag{2}$$

where y^{num} and $y^{\exp}$ are the numerical and experimental values. It is emphasized that this function is

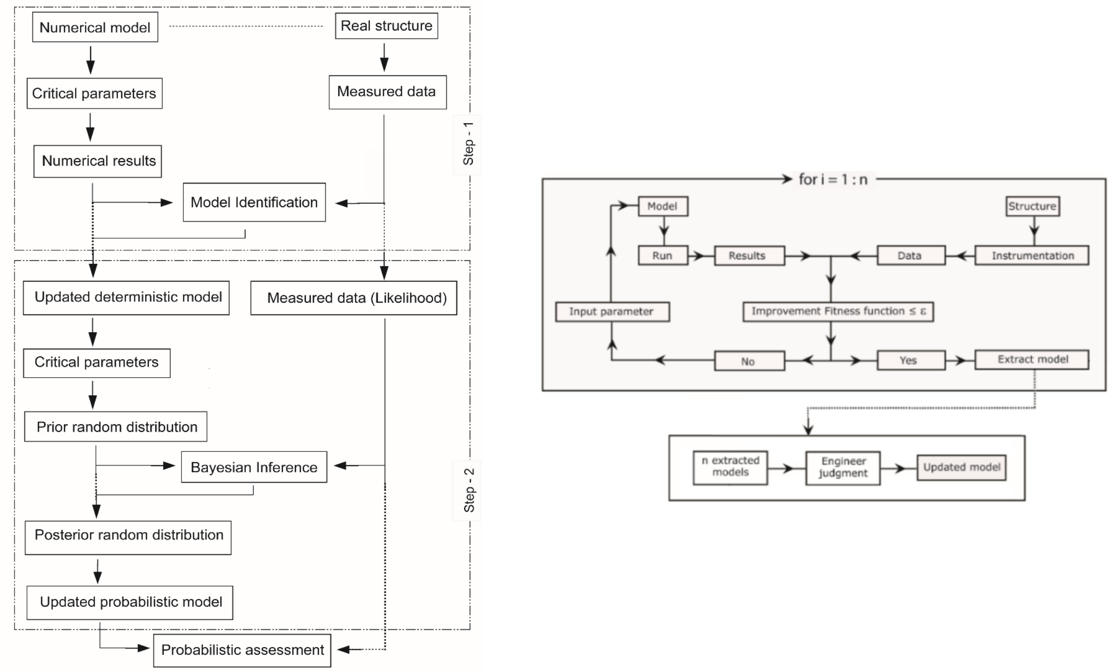

(a) (b)

Fig. 1 Probabilistic-based structural assessment framework (Matos 2013, Matos *et al*. 2015) (a) Flowchart; (b) Model identification procedure

normalized and so, it can be used with different transducers, measuring different parameters, and placed in different regions of the structure.

An optimization algorithm is used to adjust the model parameters, minimizing the distance between experimental and numerical data, given by fitness function, Eq. (2). After a thorough revision of optimization algorithms, presented in (Matos 2013), the evolutionary strategies in its plus version was chosen (Beyer and Schwefel 2002). This algorithm presents several stopping criteria (Beyer and Schwefel 2002), being the fitness function convergence criterion, expressed by Eq. (3), the most important

$$\Delta f = \left| f_{i+n} - f_i \right| \leq \varepsilon \tag{3}$$

with f_i and f_{i+n}, respectively, the fitness function values for generation i and $i+n$, and n the defined gap between two generations. When the difference between these two values is less than or equal to a pre-defined threshold value, ε, the algorithm ceases. From this procedure, those models that verify the convergence criterion are selected, being obtained a population of possible candidate models. Then, the population is filtered through a procedure, based in engineering judgment and the probability of occurrence of each model. The most likely model is the updated model.

Two sources of errors may be distinguished within the model identification procedure, namely, the experimental and numerical errors. The threshold value is then computed through the combination of these two sources of errors (Goulet *et al*. 2009, Matos 2013, Matos *et al*. 2015). Considering y as the real behavior of a quantity, $y^{\exp}$ the experimental and y^{num} the numerical value, the following relationships are then obtained through Eqs. (4)-(5)

$$y = y^{\exp} + u_{\exp} \tag{4}$$

$$y = y^{num} + u_{num} = y^{num} + (u_1 + u_2 + u_3) \tag{5}$$

being $u_{\exp}$ and u_{num}, respectively, the experimental and numerical error. This latter, can be subdivided in the following components (Goulet *et al.* 2009, Matos 2013, Matos *et al.* 2015): (a) u_1, discrepancy between the behavior of the real structure and that from the theoretical model; (b) u_2, numerical computation error of the solution of partial differential equations; and (c) u_3, inaccurate assumptions made during simulation.

The main purpose of model identification procedure is to minimize the numerator in Eq. (2), also known as residual, q. Thus, considering Eqs. (4)-(5), the residual may be expressed by Eq. (6)

$$q = \left|y^{num} - y^{\exp}\right| \Leftrightarrow q \le \left|y^{num}\right| + \left|y^{\exp}\right| \le |u| \le \left|u_{num}\right| + \left|u_{\exp}\right| \le |u_1| + |u_2| + |u_3| + \left|u_{\exp}\right| \tag{6}$$

Then, by considering Eq. (3), the convergence criterion may be simplified to Eq. (7)

$$f(q) \le u \Rightarrow \Delta f = \left|f_{i+n} - f_i\right| \Leftrightarrow \Delta f \le \left|f_{i+n}\right| + \left|f_i\right| \le \left|u_{i+n}\right| + \left|u_i\right| \le \varepsilon \tag{7}$$

being $f(q)$ the computed residual and u_i and u_{i+n}, respectively, the global uncertainty for generation i and $i+n$. Accordingly, the sum of global uncertainties from two generations corresponds to the superior limit of the threshold value.

The global uncertainty is then computed through the law of propagation of uncertainty (JCGM 2008). Accordingly, if a null correlation coefficient is considered, Eq. (8) should be used

$$u^2 = \sum_{i=1}^{n} (\partial f / \partial x_i)^2 \cdot u(x_i)^2 \tag{8}$$

where $u(x)$ is the uncertainty related to each item x, and $\partial f/\partial x$ is the partial derivative of the fitness function in order to each item x.

The global uncertainty relates to the fitness function, given in Eq. (2), which is composed by a numerical and an experimental component. The partial derivative, in relation to each term, can be obtained through $\partial f/\partial y^{num} = \partial f/\partial y^{\exp} = 1/\max(y^{\exp})$. Therefore, in this case, it is firstly necessary to compute the experimental and modeling errors in separate. The threshold value is then calculated through the fitness function convergence criterion, given by Eq. (3). In this case, the partial derivatives $\partial\Delta f/\partial u_{i+n}$ and $\partial\Delta f/\partial u_i$ are unitary.

The combination of global optimization techniques, as evolutionary strategies (Beyer and Schwefel 2002), with a model identification procedure, generally, provides a population of models. Thus, the same algorithm is run several times, as a measure to avoid the probability of underperforming results, resulting in a set of candidate optimal, or near optimal, models. The selection of the best models may be based in experience or eventually in more robust algorithms, but an expert judgment criterion is always required. Hence, an algorithm based in the probability of occurrence of each model, is used to pick the most proper model (Matos 2013, Matos *et al.* 2015). This algorithm considers that, except in some particular situations, the material and mechanical properties are close to the initial assumption.

2.2 Reliability assessment

The second step of the proposed framework, and according to Fig. 1(a), is the reliability assessment. This procedure aims to compute a reliability index, which provides information about the assessed structure condition. Accordingly, the first step consists in converting the updated numerical model into a probabilistic one by considering randomness in its parameters. In order to do so, adequate probability density functions (PDFs) are respectively assigned to model parameters, being the obtained values from model identification considered as mean values.

The random generation of model parameter values is performed with a built-in sampling technique. In this case, a LHS procedure, combined with an Iman and Conover (1982) algorithm, is employed, allowing the generation of correlated parameter values (Olsson *et al*. 2003, Shields *et al*. 2015). A nonlinear structural analysis is then developed for each set of values, being computed the corresponding failure load. Then, a distribution fitting procedure is performed to obtained set of failure loads. From this analysis, it is verified that the Normal distribution is that which best fits this set. The resistance curve, R, is respectively obtained from this procedure.

The failure probability, p_f, is then calculated by comparing the resistance and the effects of load curve, S, through a limit state function. When R and S are independent random variables, this function is given by $Z(R, S) = R - S$. In this case, the failure probability is computed by simulation methods. A reliability index, β, is then obtained through the following expression $\beta = -\Phi^{-1}(p_f)$, where Φ^{-1} is the inverse cumulative distribution function for a standard Normal distribution (Henriques 1998).

The main purpose of Bayesian techniques is the incorporation of new information into data analysis procedure, in order to reduce the statistical uncertainty (Bernardo and Smith 2004, Jacinto 2011, Matos 2013, Matos *et al*. 2015). The Bayes theorem weights the prior information with evidence provided by new data (likelihood), resulting in a posterior distribution for each model parameter. This way it will be possible to continuously update the reliability index. The final step of the reliability assessment is the comparison between the obtained reliability index and a target value, β_{target}, given in bibliography (Matos 2013, Matos *et al*. 2015).

3. Composite steel-concrete beams

3.1 Experimental tests

A set of simply supported composite beams with a span length of 4.50 m, L, and made up of a laminated steel profile connected to a solid lightweight concrete slab through headed stud steel connectors, Fig. 2(a), were tested up to failure in laboratory (Valente and Cruz 2010). Used lightweight concrete and reinforcing steel were, respectively, classified as LC 50/55 and S500B (EN 1992-1-1 2004). An IPE 120 laminated steel profile, in S275 steel (EN 1993-1-1 2004), was chosen to guarantee that the composite cross section is of class 1 (EN 1994-1-1 2004), and that the neutral axis is positioned at concrete slab when the beam is submitted to bending moments. The shear connection was provided by headed stud steel connectors, fabricated by Köco®, with steel type S235J2+C450 (EN 10025-1 2004, EN 10025-2 2004). These studs have 13 mm diameter and 50 mm length, being equally spaced along the beam. They were welded to the steel beam and later embedded in the lightweight concrete slab after casting.

One of the tested beams, designated as Beam 1, is designed for full shear connection. In this case, the cross section ultimate strength does not depend on the connection resistance (Valente and

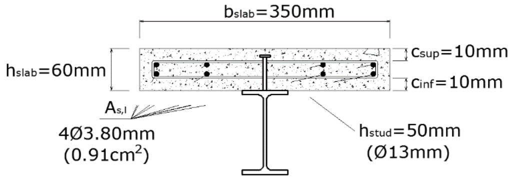

(a) Beam cross section

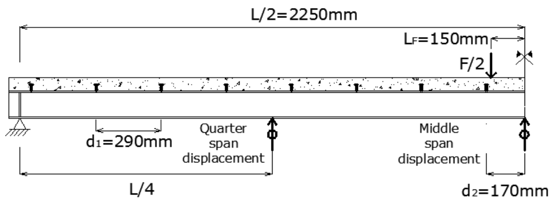

(b) Beam 1

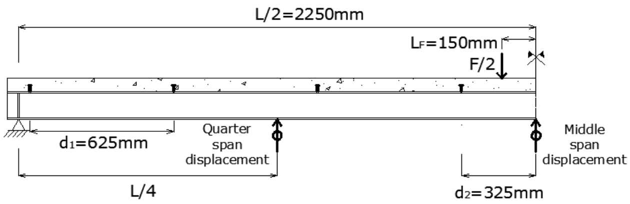

(c) Beam 2

Fig. 2 Experimental tests (Valente and Cruz 2010)

Cruz 2010). The adopted distribution is of 8 shear studs, uniformly disposed along half beam span, according to Fig. 2(b). This means that failure occurs in one of the composite section components, before the connection failure happens. The other tested beam, labeled as Beam 2, was designed for partial shear connection and presents a distribution of 4 studs in half beam span (Valente and Cruz 2010), Fig. 2(c). For this situation, a connection failure is expected.

These beams were submitted to a short-term static load with two closely spaced concentrated loads, *F*, applied on the beam mid span region, according to Figs. 2(b)-(c). A steel plate was used to divide the actuator load into two equal loads, avoiding stress concentration on beam mid span and the possibility of concrete crushing. During laboratory test, the applied load and vertical displacements at quarter and mid span were measured. The experimental procedure and the analysis of obtained results were an extensive work performed and reported by Valente (2007) and Valente and Cruz (2010). Accordingly, the pre-processing of experimental data, and all the details about the developed tests, may be consulted in those references.

Beam 1 suffered bending failure. Concrete crushed near the point load, with a longitudinal crack at mid height of concrete section, growing towards the beam mid span. The steel reinforcement near the crushing zone shows some local buckling. Beam 2 suffered a bending failure associated to a shear connection failure. Concrete crushes near the point load and, at a final stage of the test, stud failure takes place. For this beam, tensile cracks appear at bottom face of concrete slab. Additionally, the horizontal slip between steel profile and concrete slab is visible (Valente and Cruz 2010). For both beams it was verified a bending failure with yielding on the steel section lower fibbers and cracking on the concrete slab lower fibbers. The connection deformability induced a stress redistribution along the cross section, which resulted in successive changes of the neutral axis (NA) position. During load application, the NA tended to move towards the upper fibers of the cross section. The connection deformability also changed the longitudinal shear flow. Initially, the connectors positioned near the supports were more loaded than those at beam middle span, but as load increases, they began to yield and to transfer the applied load to other connectors, positioned closer to the beam middle span. With respect to Beam 2 (partial connection), where the number of shear studs along the beam is smaller, a shear connection failure was also verified, meaning that all the connectors yielded.

3.2 Numerical model

A 2D NL FEM was developed with software ATENA® (Červenka *et al*. 2009), considering both shear connection and the materials nonlinear behavior. The NL FEM is composed by a uniform quadrilateral finite element mesh, with a total number of 4934 elements, for concrete slab and steel profile, by truss elements, embedded in concrete slab, for reinforcing steel, and by interface elements, for steel to concrete connection, see Fig. 5(a). This model was used to analyze the tested composite beams behavior (Valente and Cruz 2010, Matos *et al*. 2011, 2012). Only half of the beam was modeled, taking advantage of the existent symmetry, reducing thus the computational cost. In order to do so, it was necessary to introduce horizontal supports along the symmetry line. Additionally, a vertical support was included in the model to simulate the real supports. Fig. 3(a) presents the adopted lightweight concrete stress-strain law (Červenka *et al*. 2009), defined by the following parameters: (a) tensile strength, f_{lt}; (b) fracture energy, G_{lf}; (c) compressive strength, f_{lc}; (d) elasticity modulus, E_{lc}; (e) compressive strain at compressive strength, ε_{lc}; and (f) critical displacement, w_{ld}. The stress-strain laws for reinforcement bars and laminated steel profile are respectively given in Figs. 3(b)-(c) (Červenka *et al*. 2009). These laws are characterized by the following parameters: (a) elasticity modulus, $E_{s,l}$ and $E_{s,p}$; (b) yield strength, $\sigma_{y,l}$ and $\sigma_{y,p}$; (c) reinforcing steel limit strain, $\varepsilon_{lim,l}$; (d) reinforcing steel limit strength, $\sigma_{u,l}$; (e) steel profile hardening modulus, H_p. The initial values for steel profile parameters are given at EN 1993-1-1 (2010), while for steel reinforcement, they are provided at EN 1992-1-1 (2004). Regarding the lightweight concrete, these values are obtained from expressions given at EN 1992-1-1 (2004), considering an initial estimate for its density. In this case a value of 1811.50 kg/m^3 was respectively assigned to this parameter (Valente 2007). Some lightweight concrete parameter values, such as fracture energy and critical displacement, were obtained from specialized bibliography (Červenka *et al*. 2009). The majority of these values are mean values. In some occasions this does not happens, being necessary to obtain them from the Probabilistic Model Code (JCSS 2001).

The concrete slab and steel profile connection, provided by headed stud steel connectors, is modeled with an interface material model (Červenka *et al*. 2009). This model is based on a Mohr-Coulomb criterion with tension cut-off. This law is given in terms of shear, τ, and normal stresses, σ. According to Fig. 4(a), the dry friction, ϕ, is considered to be very low and therefore the initial failure corresponds to the moment when cohesion value, c, is reached. For shear stresses, and for positive slip, Δu_T, this law is characterized by an initial shear stiffness, K_{TT}, until the Mohr-Coulomb criterion is reached, and then it presents a minimum shear stiffness, $K_{TT,min}$, that is 1% of

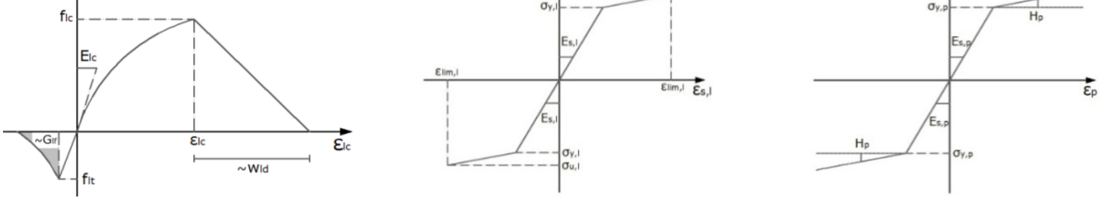

(a) (b) (c)

Fig. 3 Stress-strain law (Červenka *et al*. 2009): (a) concrete; (b) reinforcing steel; (c) steel profile

K_{TT}, Fig. 4(b). This behavior tries to replicate the relation between shear stress and slip at steel to concrete interface, verified in push-out tests. For normal stresses, and for positive uplifts, Δu_N, it is defined by an initial normal stiffness, K_{NN}, until the tensile strength, f_t, is reached. Once attained, the normal stress is reduced to 0, being this law defined by a minimum normal stiffness, $K_{NN,min}$, that is 1% of K_{NN}, Fig. 4(c).

Both tensile strength and normal stiffness are assumed to present high values in order to guarantee that the connection is working when submitted to normal stresses. The cohesion value

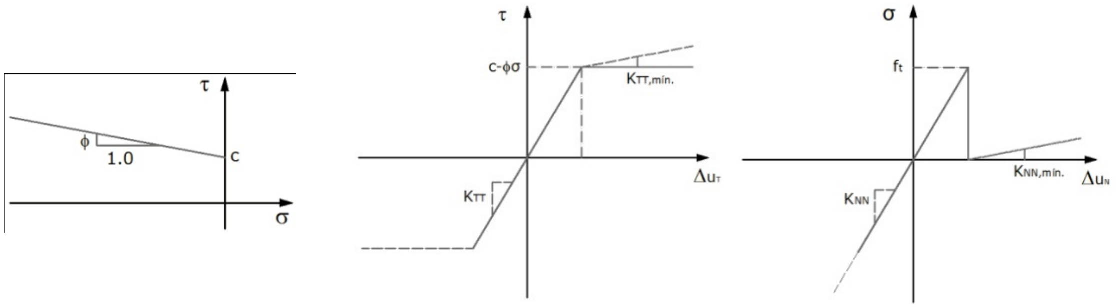

(a) (b) (c)

Fig. 4 Interface law (Červenka *et al*. 2009): (a) failure criteria; (b) shear stress and slip; (c) normal stress and uplift

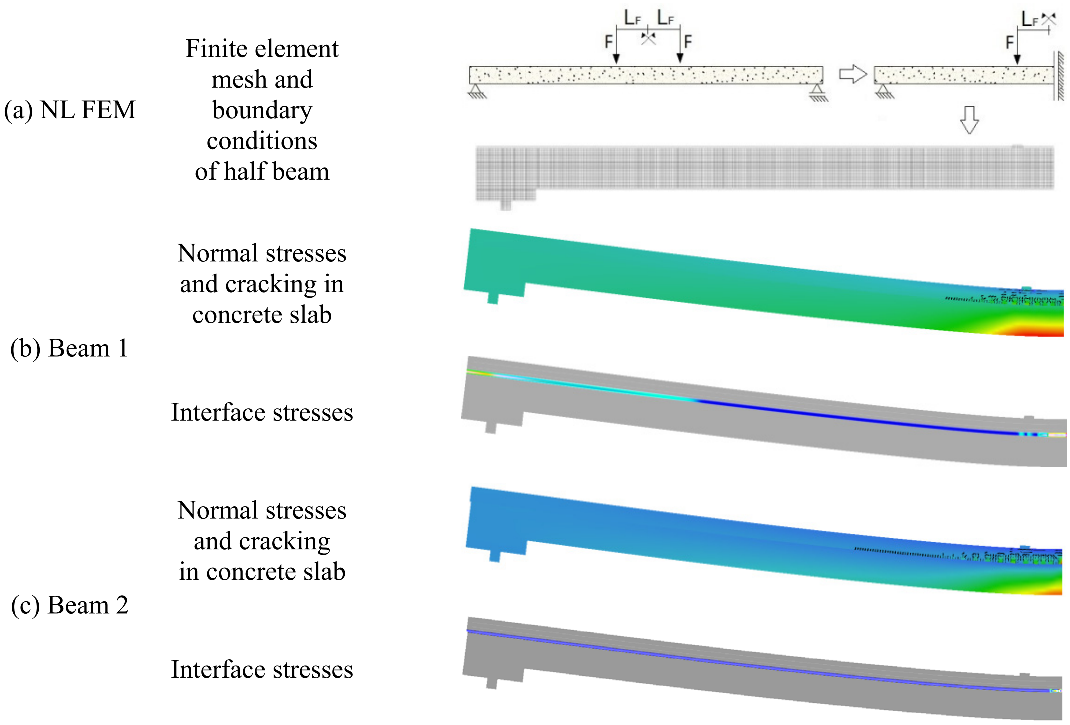

Fig. 5 Numerimerical model (top: Beam 1 / bottom: Beam 2) (Matos 2013): (a) failure mechanism; (b) interface stresses

depends from the connection maximum load capacity, which is computed based on expressions from EN 1994-1-1 (2004), and considering both the lightweight concrete and the headed stud material and geometric parameters values. Then, the mean value of the connection maximum load capacity is multiplied by the ratio number of studs per beam length, and divided by the interface width, being calculated a mean value for the cohesion interface parameter. The shear stiffness is obtained from a similar way as for cohesion, but now considering the connection stiffness. In this case, a mean value of 220 kN/mm is estimated from the literature (Valente 2007, Valente and Cruz 2010).

Fig. 5(a) provides the deformation, crack pattern in concrete slab and horizontal strains of analyzed Beam 1, for chosen numerical model and considering the initial values. This figure also shows the interface stresses between concrete slab and steel profile. It is possible to observe that cohesion value, in blue color, is only reached in a small region of the interface. In Beam 2, Fig. 5(b), the obtained failure mode is bending with concrete crushing and yielding of steel profile, together with a lack of capacity to redistribute more shear stress as the cohesion value is reached along the whole steel-concrete interface (Červenka *et al*. 2009). It is verified for both that obtained behavior is similar to experimental one. A higher failure load is obtained for Beam 1, full shear connection, being verified a full redistribution of shear stresses. In Beam 2, there is also a total redistribution of shear stresses, but the shear strength is lower, less shear studs disposed, and therefore earlier attained.

3.3 Sensitivity analysis

It is known that within the probabilistic-based assessment framework, the computational cost increases with the number of variables to be identified. Therefore, it is important to select those who are critical. This can be done by performing a sensitivity analysis. Within this analysis, the importance measure of each model parameter is evaluated by adding or subtracting a standard deviation value to the studied parameter mean (or nominal) value, and keeping all the other parameters fixed. Then, for each set of parameter values, a nonlinear analysis is developed, being applied the Eq. (1) to compute the assessed parameter importance measure. These steps are repeated to all model parameters. The obtained importance measure values are then normalized with relation to the maximum value, being the results presented in a bar plot. In this case, if obtained importance measure value is equal or higher than 10%, b_{lim}, the parameter will be considered as critical (Matos 2013). Two sensitivity analyses are developed, one for service phase, Fig. 6, and other until failure load, Fig. 7.

From the analysis performed in service region, it is possible to identify as critical parameters: (a) concrete elasticity modulus, E_{lc}; (b) steel profile elasticity modulus, $E_{s,p}$; (c) slab width, b_{slab}; (d) slab height, h_{slab}; (e) steel profile web thickness, b_{web}; (f) steel profile height, h_{web}; (g) steel profile superior flange width, $b_{fl,sup}$; and (h) steel profile inferior flange thickness, $h_{fl,inf}$. Accordingly, from 26 possible parameters, only 8 of them were considered, reducing the computational cost.

From the performed analysis in failure region, it is concluded that critical parameters identified during the analysis for service phase still present a significant influence in structural behavior. In this evaluation, all concrete parameters become critical, mainly those that describe its behavior in compression. These parameters present a higher impact, as bending failure with concrete crushing is identified. In the same way, steel profile parameters, with exception of hardening modulus, H_p, are critical as steel material yields before concrete crushing. In respect to interface parameters, for higher loads, the maximum stress at interface element is reached in some regions. Consequently, the cohesion parameter, c, becomes an important parameter too. In a general way, the geometric parameters related to concrete slab and laminated steel profile dimensions, with exception of inferior flange width, $b_{fl,inf}$, present a high influence on structural behavior. In this situation, from 26 possible initial parameters, only 16 were considered in the study.

The sensitivity analysis performed for Beam 2 is identical to that developed for Beam 1. The only difference consists in some of the interface parameters, namely, cohesion, c, and shear stiffness, K_{TT}, for which the initial values are different, resulting from the specific number of shear studs disposed in each beam. The importance of these two parameters increased, as expected, but still only cohesion in the analysis up to failure is considered as critical.

Zona *et al*. (2006) performed a sensitivity analysis on composite structures, more specifically in continuous steel-concrete girders, for both monotonic and cyclic loads. The following parameters were studied with detail within this analysis: (i) steel profile elasticity modulus; (ii) steel profile yield strength; (iii) steel profile hardening modulus; (iv) concrete elasticity modulus; (v) concrete compressive strength; (vi) steel reinforcement elasticity modulus; (vii) steel reinforcement yield strength; and (viii) shear connection tensile strength. For monotonic load case, and for the service region, the authors pointed out the concrete elasticity modulus and steel profile elasticity modulus as the most influent parameters. In respect to failure region, the most important parameters were the steel profile yield strength and hardening modulus, the concrete compressive strength, the steel reinforcement yield strength and the shear connection tensile strength. Although in the present

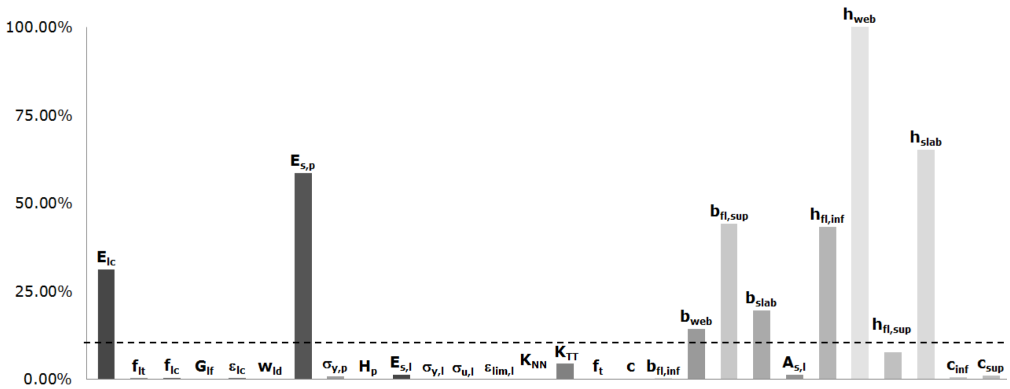

Fig. 6 Importance measure (in service) (Matos 2013)

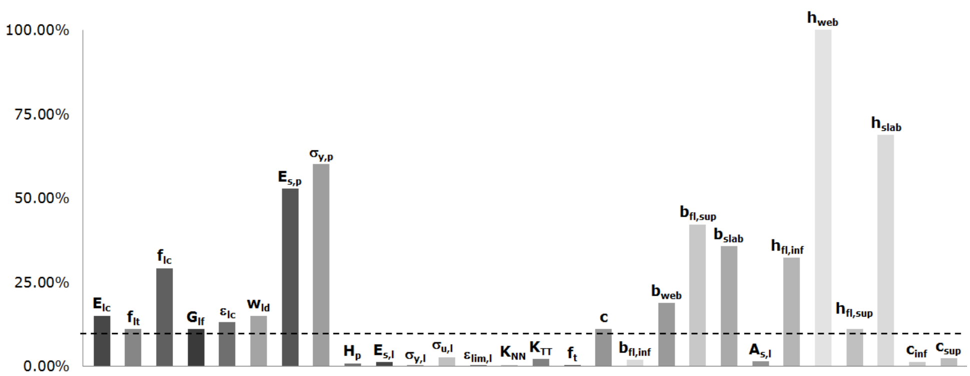

Fig. 7 Importance measure (up to failure) (Matos 2013

study more parameters were assessed, namely the geometric parameters, it is possible to identify the following similarities: (i) for service region, the same parameters were identified as critical in both studies; (ii) for failure region, the present study indicates that the steel profile hardening modulus, the steel reinforcement yield strength and the shear connection tensile strength are not critical. Instead, the steel profile elasticity modulus and the concrete elasticity modulus are considered as critical. This is somehow justified by the obtained failure mode, and by the developed sensitivity analysis procedure. Nevertheless, it is possible to verify that the obtained results by Zona *et al*. (2006) are similar to those from the present sensitivity analysis, being very interesting to verify that different finite element models and sensitivity analysis procedures lead to identical results.

3.4 Model identification

Once the numerical model and critical parameters are obtained, the following step consists in the application of proposed model identification methodology, Fig. 1(b). In this situation, the fitness function, Eq. (2), is the quadratic sum of two independent components, the degree of approximation between experimental and numerical load for each registered quarter and mid span displacements, δ, i.e., the fitness function characterizes the approximation between numerical and experimental values for applied load. Then, the threshold value, ε, to be used in fitness function convergence criterion is computed. In order to do it, the identification of experimental, $u_{\exp}$, and numerical, u_{num}, sources of errors should be firstly developed, Table 1.

Table 1 Errors, sources and quantification

Error source	Quantification method		Error [%]
Experimental	Sensor accuracy	Manufacturer (includes cable and acquisition equipment losses)	0.20 (displacement transducer)
	Stability	Static load test (no fatigue problems detected)	→ 0.00
	Robustness	Short term test (environmental effects neglected)	→ 0.00
	Load positioning	Test assembly perfectly controlled	→ 0.00
	Load intensity	Manufacturer (includes cable and acquisition equipment losses)	0.10 (load cell)
Numerical	Finite element method	Based on preliminary study (by comparing to a refined mesh model)	0.34 ($\delta^{1/4}$ vs. F) [a]; 0.74 ($\delta^{1/2}$ vs. F) [a]
	Inaccurate assumptions	Based on preliminary study (by comparing to a short load step model)	0.70 ($\delta^{1/4}$ vs. F) [a]; 1.42 ($\delta^{1/2}$ vs. F) [a]
	Model exactitude	Model "as built"	→ 0.00
	Considered hypothesis	Other hypothesis are negligible	→ 0.00

[a] Computed values for the analysis up to failure load (JCSS 2001)

Table 2 provides the experimental and the numerical uncertainty computation, through the law of propagation of uncertainty (JCGM 2008), for the analysis until failure load (Beam 1). The standard error is obtained considering that a uniform PDF, type B, is respectively assigned to each component error j (JCGM 2008). The partial derivative of each error, with respect to each component of error, is unitary. Then, it is possible to compute the fitness function uncertainty for each fitness function component i, Table 3, through the law of propagation of uncertainty (JCGM 2008). In order to do so, it is required to calculate the fitness function partial derivative in relation to each error source. The fitness function value improvement uncertainty and the corresponding threshold value computation, supported on the law of propagation of uncertainty (JCGM 2008), is respectively provided at Table 4.

The same laboratory equipment and numerical model was adopted for Beam 1 and 2. Consequently, the only difference on threshold values computation remains on the derivative of

Table 2 Computation of experimental and numerical uncertainty (JCGM 2008)

	Component, i		δ-$F_{1/4}$	δ-$F_{1/2}$
Experimental	Error, j	[%]	0.10 (load cell, Table 1)	0.10 (load cell, Table 1)
	Standard error, $u_{\exp,ij}$	[-]	$\frac{0.10}{100}\times\frac{1}{\sqrt{3}}=5.77\times10^{-4}$	$\frac{0.10}{100}\times\frac{1}{\sqrt{3}}=5.77\times10^{-4}$
	$\partial y^{\exp}/\partial u_{\exp,ij}$	[kN]	1	1
	Experimental error, $u_{\exp,i}$	[kN]	$\sqrt{1^2\times(5.77\times10^{-4})^2}=5.77\times10^{-4}$	$\sqrt{1^2\times(5.77\times10^{-4})^2}=5.77\times10^{-4}$
Numerical	Error, j	[%]	0.34 (finite element method, Table 1) 0.70 (inaccurate assumptions, Table 1)	0.74 (finite element method, Table 1) 1.42 (inaccurate assumptions, Table 1)
	Standard error, $u_{num,ij}$	[-]	$\frac{0.34}{100}\times\frac{1}{\sqrt{3}}=0.20\times10^{-2}$ $\frac{0.70}{100}\times\frac{1}{\sqrt{3}}=0.40\times10^{-2}$	$\frac{0.74}{100}\times\frac{1}{\sqrt{3}}=0.43\times10^{-2}$ $\frac{1.42}{100}\times\frac{1}{\sqrt{3}}=0.82\times10^{-2}$
	$\partial y^{num}/\partial u_{num,ij}$	[kN]	1	1
	Numerical error, $u_{num,i}$	[kN]	$\sqrt{1^2\times(0.20\times10^{-2})^2+1^2\times(0.40\times10^{-2})^2}=4.49\times10^{-3}$	$\sqrt{1^2\times(0.43\times10^{-2})^2+1^2\times(0.82\times10^{-2})^2}=9.25\times10^{-3}$

Table 3 Uncertainty calculation for each fitness function component (JCGM 2008)

Component, i	$\partial f/\partial y^{\exp,ik}$ [kN^{-1}]	$\partial f/\partial y^{num,ik}$ [kN^{-1}]	Fitness uncertainty, $u_{f,ik}$ [-]	$\partial f/\partial f_{ik}$ [-]	Fitness uncertainty, $u_{f,i}$ [-]
δ-$F_{1/4}$	4.20×10^{-2}	4.20×10^{-2}	$\sqrt{(4.20\times10^{-2})^2\times(5.77\times10^{-4})^2+(4.20\times10^{-2})^2\times(4.49\times10^{-3})^2}=1.90\times10^{-4}$	1	$\sqrt{1^2\times(1.90\times10^{-4})^2+1^2\times(3.88\times10^{-4})^2}=4.32\times10^{-4}$
δ-$F_{1/2}$	4.20×10^{-2}	4.20×10^{-2}	$\sqrt{(4.20\times10^{-2})^2\times(5.77\times10^{-4})^2+(4.20\times10^{-2})^2\times(9.25\times10^{-3})^2}=3.88\times10^{-4}$	1	

the fitness function with respect to experimental and numerical results, as the maximum experimental load is different in this situation, $\partial f/\partial y^{num} = \partial f/\partial y^{\exp} = 1/\max(y_i^{\exp}) = 4.20 \times 10^{-1}$ kN^{-1}, for Beam 1, and equal to 4.70×10^{-1} kN^{-1}, for Beam 2. Table 4 presents obtained threshold values, for service and up to failure, for both beams.

This means that, for instance, for Beam 1, if the improvement in minimum fitness function value, until failure load, of a population from two generations separated of a specified gap, n, is, respectively, less than or equal to 0.12% than the algorithm stops, as the fitness function convergence criteria is achieved. In this case it was considered a gap of 100 (Matos 2013). This means that it is not meaningful to improve the fitness function of a value that is less than or equal to the precision itself. Obtained results from model identification procedure are given in Table 5.

Obtained values from model identification until failure load indicate a concrete material quality close to expected and a steel material quality higher than predicted. The initial estimate for steel-

Table 4 Threshold value calculation (JCGM 2008)

$\partial\Delta f/\partial f_i$	$\partial\Delta f/\partial f_{i+n}$	Improvement uncertainty, $u_{\Delta f}$	Coverage factor, k	Threshold value, ε		Threshold value for both beams, ε	
[-]	[-]	[-]	[-]	[-]	[%]	Beam 1	Beam 2
1	1	$\sqrt{\begin{array}{l}1^2 \times (4.32\times10^{-4})^2 + \\ 1^2 \times (4.32\times10^{-4})^2\end{array}} = 6.11\times10^{-4}$	2	1.22×10^{-3}	0.12	Service: 0.08% Failure: 0.12%	Service: 0.09% Failure: 0.25%

Table 5 Model identification results

Parameter		PDF	Initial value	Service		Failure	
			Beams 1 (and 2)	Beam 1	Beam 2	Beam 1	Beam 2
E_{lc}	[GPa]	Normal	25.09	30.00	30.00	23.71	26.73
f_{lt}	[MPa]	Normal	3.67	-	-	3.56	3.16
f_{lc}	[MPa]	Normal	58.00	-	-	59.19	58.93
G_{lf}	[N/m]	Normal	91.75	-	-	91.18	91.67
ε_{lc}	[‰]	Normal	2.20	-	-	2.69	2.80
w_{ld}	[m]	Normal	1.50×10^{-3}	-	-	1.51×10^{-3}	1.71×10^{-3}
$E_{s,p}$	[GPa]	Normal	210.00	230.00	216.51	215.65	199.75
$\sigma_{y,p}$	[MPa]	Normal	293.50	-	-	297.98	350.00
c	[MPa]	Normal	2.95 (and 1.47)	-	-	3.00	1.55
b_{web}	[mm]	Normal	4.40	4.20	4.80	5.22	4.79
$b_{fl,sup}$	[mm]	Normal	64.00	63.00	63.74	63.95	63.81
b_{slab}	[mm]	Normal	350.00	348.63	354.91	353.83	349.56
$h_{fl,inf}$	[mm]	Normal	6.60	7.60	7.60	6.64	6.50
h_{web}	[mm]	Normal	106.80	106.04	106.92	106.89	106.86
$h_{fl,sup}$	[mm]	Normal	6.60	-	-	7.21	6.60
h_{slab}	[mm]	Normal	60.00	61.26	59.49	62.14	59.85

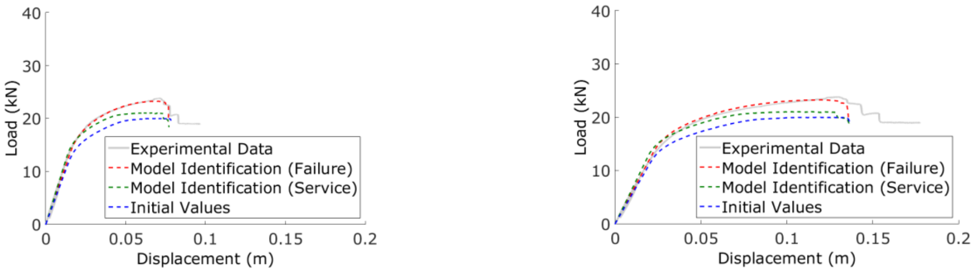

(a) (b)

Fig. 8 Numerical results (Matos 2013): (a) Beam 1; (b) Beam 2

Table 6 Minimum fitness function values

Numerical model	Service				Failure			
	Beam 1		Beam 2		Beam 1		Beam 2	
	Value [%]	Improvement [%]	Value [%]	Improvement [%]	Value [%]	Improvement [%]	Value [%]	Improvement [%]
Initial values	4.65	-	3.85	-	19.35	-	20.43	-
Model identification	0.80	82.80	0.95	75.30	2.13	89.00	5.82	71.50

concrete interface is confirmed by model identification until failure load. Steel profile and concrete slab dimensions are close to those expected in design for both model identification procedures and for most of assessed parameters.

In Figs. 8(a)-(b), the applied load is plotted against the mid span displacements, respectively, for Beam 1 and 2, for measured data and for numerical results, considering the initial values, and those from model identification in service phase and until failure load. By studying both figures it is possible to conclude that model identification until failure load, presents the numerical curve that best fits the experimental data.

Table 6 indicates the minimum fitness function values obtained by considering the initial values and those from model identification. It is verified that obtained value from model identification in

Table 7 Failure load, F_R, and corresponding vertical displacement, δ_R

Obtained values		Failure load				Vertical displacement			
		Beam 1		Beam 2		Beam 1		Beam 2	
		Value [kN]	Error [%]*	Value [kN]	Error [%]*	Value [mm]	Error [%]*	Value [mm]	Error [%]*
Experimental values		23.86	-	21.20	-	129.80	-	239.50	-
Initial values		19.99	16.22	17.18	18.97	122.66	5.50	262.76	9.71
Model identification	Service	21.06	11.74	17.41	17.88	105.03	19.08	244.06	1.90
	Failure	23.26	2.51	20.04	5.47	119.79	7.71	273.70	14.28

* Comparing with the real failure load and correspondent vertical displacement

service phase is lower than that determined until failure. In fact, in service region, experimental and numerical results are closer than those for higher applied loads. Nevertheless, for these two situations the applied methodology revealed an important improvement of this value.

Table 7 indicates the failure load, F_R, and the corresponding vertical displacement, δ_R, measured at beam middle span. Obtained values from model identification until failure load are, in most situations, those that present a lower error, as when applying the methodology in service phase, the model identification is performed for this region, not being possible to guarantee the curve fitting for failure region. Obtained error for the situation of model identification until failure load is, for most situations, less than 10%, which is considered to be very good, being thus the most accurate model.

3.5 Reliability assessment

At this point a deterministic numerical model was developed and adjusted to obtained experimental data, through a model identification procedure. The next step of this methodology consists in computing a resistance statistical distribution, supported in a reliable probabilistic numerical model, Fig. 1(a) (Matos *et al*. 2011, Matos *et al*. 2012). This model is obtained by considering randomness in some input parameters, such as those related to concrete slab, steel profile and interface between these two components.

The majority of the adopted statistical distributions for model parameters, as well as the corresponding correlation values, are obtained from the Probabilistic Model Code (JCSS 2001). However, there are some parameters for which the existing data is few, such as some lightweight concrete parameters like the fracture energy, with information solely in specialized references (Leming 1988, Valum and Nilsskog 1999, EuroLightCon 2000, Nowak *et al*. 2008), and the interface cohesion, i.e., the connection maximum load capacity, for which it was possible to find some material in the work of Valente (2007) and Roik *et al*. (1989). From all distribution types, the Normal distribution is the most used. As mean value, μ, it was considered the initial values or those from model identification in service phase and until failure load, being the standard deviation, σ, obtained from the literature. These values are given at Table 11.

In some situations, when there is complementary data (or likelihood), a Bayesian inference approach can be used (Bernardo and Smith 2004, Matos 2013). An informative and a non-informative (Jeffrey's) prior were used in the Bayesian inference procedure with the aim of computing the posterior distribution, being the considered posterior distribution that which presents the lowest standard deviation value. Once each critical parameter PDF is defined, the next step consists in the random generation of these parameter values. This procedure is based in a LHS technique (Olsson *et al*. 2003). The correlation between critical random variables is assured by the Iman and Conover (1982) algorithm. A set of values are respectively obtained from the probabilistic analysis. These values are then statistically processed and fitted to a Normal distribution, in order to compute the resistance curve.

In this case, complementary tests were developed at laboratory to characterize the material and interface parameters as to provide means to quantify the accuracy of the model identification procedure, and to increase the existing knowledge about these parameters (Valente 2007). With respect to concrete, the compressive strength and elasticity modulus were obtained in uniaxial compression tests, and both the concrete tensile strength and fracture energy in bending tests. Accordingly, from the whole set of performed tests, only 10 observations for compressive strength and elasticity modulus, and 5 observations for tensile strength and fracture energy were taken into account. The concrete specimens were produced at the same time of the corresponding composite beam and tested at the same date (31 days for beam 1, and 35 days for beam 2). In order to characterize the steel material used in stud connectors, reinforcement bars and laminated profile, uniaxial tensile tests were performed. Due to the small size of the headed studs (13 mm diameter and 50 mm length), no experimental test was done on the steel properties of these connecting devices. However, the obtained values in tested studs with higher diameters, also produced by Köco®, were considered. From the entire set of tests, only the results from 8 specimens of headed studs, 3 specimens of reinforcement bars, and 3 specimens of laminated steel profile were considered. Additionally, some push-out tests were developed to study the steel-concrete connection behavior. During these tests it was used the same type of lightweight concrete and an identical type of shear connectors as that used in tested beams. Tested proofs were cast at the same time of the corresponding beam and also tested at same date. From the developed push-out tests it was obtained the connection maximum load capacity and stiffness, being then computed the cohesion and the shear stiffness for each beam type. In this case, only 5 observations were considered. The pre-processing of obtained data, as well as any more detail about these tests, can be consulted in Valente (2007) and in Valente and Cruz (2010). A statistical analysis was performed for each parameter and the corresponding mean and standard deviation values are provided in Table 8.

Obtained values for concrete parameters are close to initial values. The exception goes to fracture energy, who obtained lower values than the initial ones. Coefficients of variation, CV, are all less than 10% which indicates that the variability of such parameters is small. Regarding steel parameters, obtained values indicate that used material is of better quality than expected in design. Obtained CV values are, in general, lower than 5% which indicates a small variation of these properties. Table 8 also presents the push-out tests results for both beams, respectively, with full

Table 8 Concrete, steel and interface parameters (Valente and Cruz 2010, Matos 2013)

	Parameter		PDF	Initial value	Mean value, μ	Standard deviation, σ
Concrete	Elasticity modulus, E_{lc}	[GPa]	Normal	25.09	24.81	2.23
	Tensile strength, f_{lt}	[MPa]	Normal	3.67	3.78	0.16
	Compressive strength, f_{lc}	[MPa]	Normal	58.00	57.96	4.64
	Fracture energy, G_{lf}	[N/m]	Normal	91.75	78.42	1.83
Steel - laminated profile	Yield strength, $\sigma_{y,p}$	[MPa]	Normal	293.50	335.67	9.10
	Hardening modulus, H_p	[GPa]	Normal	1.04	0.72	0.09
Steel - reinforcement	Yield strength, $\sigma_{y,l}$	[MPa]	Normal	560.00	583.41	8.02
	Ultimate strength, $\sigma_{u,l}$	[MPa]	Normal	604.80	606.06	8.32
Steel - Studs	Tensile strength, f_t	[MPa]	Normal	-	567.57	18.95
Beam 1 - Interface	Shear stiffness, K_{TT}	[MPa] (*per mm*)	Normal	12.22	10.89	1.27
	Cohesion, c	[MPa]	Normal	2.95	3.15	0.09
Beam 2 - Interface	Shear stiffness, K_{TT}	[MPa] (*per mm*)	Normal	6.10	5.44	0.63
	Cohesion, c	[MPa]	Normal	1.47	1.58	0.05

(Beam 1) and partial connection (Beam 2). As the considered value of maximum applied load (per connector) and of connection stiffness is the same, the main difference between both beams consists in the number of used studs (EN 1994-1-1 2004).

From characterization tests, new information regarding material and interface parameters is available. These observations can be used, within a Bayesian inference procedure, to update the prior distributions which are those that have, as a mean value, the initial parameter value or that obtained from model identification (Table 11). Used Bayesian inference methodology is exemplified with an application to the lightweight concrete compressive strength, considering a Jeffrey's and a conjugate prior. The choice of a prior distribution is a crucial step in Bayesian inference. The use of a non-informative prior is particularly helpful when no prior information is available, but it is always required to verify if the computed posterior distribution is proper (Bernardo and Smith 2004). A typical non-informative prior is the Jeffrey's prior, which commonly results in a proper posterior distribution. When there is any information regarding the parameter of interest, the informative prior may be used instead. Conjugacy is the property of a posterior distribution to belong to the same family of the prior distribution (Bernardo and Smith 2004). Conjugate families are thus useful, from a mathematical perspective, since the posterior distribution follows a known parametric form. Table 9 presents both prior distributions considered in the present study. In this case, it is considered a conjugate prior with a mean value of 58,00 MPa, initial value, and a standard deviation of 5,80 MPa (Table 11). The likelihood represents the observations about the assessed parameter. In this situation, it is obtained from uniaxial compressive test specimens, with a mean value of 57,96 MPa and a standard deviation of 4,64

Table 9 Used formula to compute the posterior distribution values for lightweight concrete compressive strength

Jeffrey's	Conjugate
Prior	
$p(\mu,\sigma^2) \propto \frac{1}{\sigma^2}, -\infty < \mu < \infty, \quad \sigma^2 > 0$	$\mu \mid \sigma^2 \to N\left(\mu_0, \frac{\sigma^2}{n_0}\right) \Rightarrow \mu \mid \sigma^2 \to N\left(58, \frac{\sigma^2}{10}\right)$ $\frac{1}{\sigma^2} \to \text{gamma}\left(\frac{v_0}{2}, \frac{S_0}{2}\right) \Rightarrow \frac{1}{\sigma^2} \to \text{gamma}(4.5, 151.38)$
Posterior	
$\mu \mid \sigma^2,\ X \to N\left(\bar{x}, \frac{\sigma^2}{n_0}\right) \Rightarrow \mu \mid \sigma^2,$ $X \to N\left(57.96, \frac{\sigma^2}{10}\right)$	$\mu \mid \sigma^2 \to N\left(\mu_1, \frac{\sigma^2}{n_1}\right) \Rightarrow \mu \mid \sigma^2 \to N\left(57.98, \frac{\sigma^2}{20}\right)$
$\frac{(n-1)\cdot s^2}{\sigma^2} \to \chi^2_{n-1} \Rightarrow \frac{4187.38}{\sigma^2} \to \chi^2_{n-1}$	$\left.\frac{1}{\sigma^2}\right\vert x \to \text{gamma}\left(\frac{v_1}{2}, \frac{S_1}{2}\right)$ $\Rightarrow \left.\frac{1}{\sigma^2}\right\vert x \to \text{gamma}(9.5, 496.90)$

Table 10 Posterior distributions, considering different prior distributions, for lightweight concrete compressive strength

Parameter	Jeffrey's	Conjugate
μ_0	-	58.00
σ_0	-	5.80
μ_1	57.97	57.98
$\sigma(\mu_1)$	1.74	1.20
σ_1	5.34	5.28
$\sigma(\sigma_1)$	1.44	1.07
μ_{pop}	57.97	57.98
σ_{pop}	5.82	5.50

Table 11 Parameter values

Parameter	PDF	Initial value *		Model identification (in service) *		Model identification (at failure) *	
		μ	σ	μ	σ	μ	σ
Beam 1							
E_{lc} [GPa]	Normal	25.09 (24.81)	2.51 (2.20)	30.00 (24.81)	3.00 (2.20)	23.71 (24.81)	2.37 (2.20)
f_{lt} [MPa]	Normal	3.67 (3.78)	0.73 (0.28)	3.67 (3.78)	0.73 (0.28)	3.56 (3.78)	0.71 (0.28)
f_{lc} [MPa]	Normal	58.00 (57.98)	5.80 (5.50)	58.00 (57.98)	5.80 (5.50)	59.19 (57.98)	5.92 (5.50)
G_{lf} [N/m]	Normal	91.75 (78.33)	9.18 (7.13)	91.75 (78.33)	9.18 (7.13)	91.18 (78.33)	9.12 (7.13)
$\sigma_{y,p}$ [MPa]	Normal	293.50 (337.61)	14.68 (37.75)	293.50 (337.61)	14.68 (37.75)	297.98 (337.61)	14.90 (37.75)
c [MPa]	Normal	2.95 (3.12)	0.37 (0.10)	2.95 (3.12)	0.37 (0.10)	3.00 (3.08)	0.38 (0.10)
Beam 2							
E_{lc} [GPa]	Normal	25.09 (24.81)	2.51 (2.21)	30.00 (24.81)	3.00 (2.21)	26.73 (24.81)	2.67 (2.21)
f_{lt} [MPa]	Normal	3.67 (3.78)	0.73 (0.28)	3.67 (3.78)	0.73 (0.28)	3.16 (3.78)	0.63 (0.28)
f_{lc} [MPa]	Normal	58.00 (58.31)	5.80 (5.02)	58.00 (58.31)	5.80 (5.02)	58.93 (58.31)	5.89 (5.02)
G_{lf} [N/m]	Normal	91.75 (78.33)	9.18 (7.13)	91.75 (78.33)	9.18 (7.13)	91.67 (78.33)	9.17 (7.13)
$\sigma_{y,p}$ [MPa]	Normal	293.50 (337.61)	14.68 (37.75)	293.50 (337.61)	14.68 (37.75)	350.00 (342.81)	17.50 (24.63)
c [MPa]	Normal	1.47 (1.56)	0.18 (0.07)	1.47 (1.56)	0.18 (0.07)	1.55 (1.56)	0.19 (0.07)

* Bayesian inference values are given between brackets

Table 12 Failure load, F_R

Numerical model	PDF	Beam 1		Beam 2	
		μ [kN]	σ [kN]	μ [kN]	σ [kN]
Initial values	Normal	19.00	2.21	16.49	2.02
Initial values + Bayesian inference	Normal	22.76	2.50	19.14	1.58
Model identification (service)	Normal	20.47	1.76	18.16	1.96
Model identification (service) + Bayesian inference	Normal	23.87	2.28	20.86	1.55
Model identification (failure)	Normal	21.89	2.56	19.35	2.54
Model identification (failure) + Bayesian inference	Normal	24.42	2.49	19.56	0.92

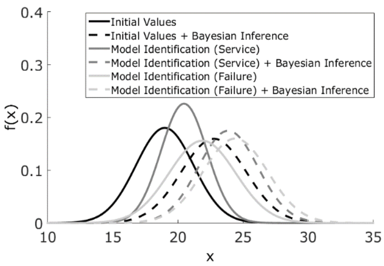

(a)

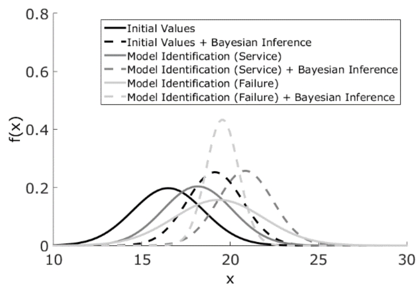

(b)

Fig. 9 Failure load, F_R (Matos 2013): (a) Beam 1; (b) Beam 2

MPa (Table 8). In Table 9 it is also provided the most important formula for the computation of the posterior distribution values. A more detailed explanation is given at Matos (2013). Table 10 presents the lightweight concrete compressive strength values, obtained from the application of the Bayesian inference analysis.

In this case, as the conjugate prior gives a lower standard deviation value for the lightweight concrete compressive strength, it will be this distribution to be used in a further probabilistic analysis. Table 11 presents, between brackets, the Bayesian inference results for all parameters (Matos 2013). In a general way, the Bayesian updating provided mean values close to initial values and those from model identification. Moreover, and with exception of steel profile yield strength, for which obtained experimental data is far from numerical results, the Bayesian inference procedure reduced the standard deviation values.

Then, a set of failure load, F_R, values is respectively computed through the probabilistic analysis. A Normal PDF, which represents the structural resistance, is then adjusted to this set. Obtained resistance PDF parameter values for Beam 1 and 2 is given in Table 12.

From the analysis of obtained results, it is possible to conclude that: (1) The mean value increases as model identification procedures are applied; (2) The Bayesian inference approach increases the mean and reduces the CV of obtained resistance PDF. Figs. 9(a)-(b) represents the obtained resistance PDF, for Beam 1 and 2, respectively, whose parameter values (mean and standard deviation) are given in Table 12.

Table 13 Safety assessment

Numerical model	p_f		β	
	Beam 1	Beam 2	Beam 1	Beam 2
Initial values	1.05×10^{-3}	2.53×10^{-3}	3.07	2.81
Initial values + Bayesian inference	2.90×10^{-4}	8.32×10^{-4}	3.44	3.15
Model identification (service)	5.44×10^{-4}	1.31×10^{-3}	3.27	3.00
Model identification (service) + Bayesian inference	1.82×10^{-4}	4.51×10^{-4}	3.57	3.31
Model identification (failure)	4.06×10^{-4}	1.04×10^{-3}	3.34	3.08
Model identification (failure) + Bayesian inference	1.57×10^{-4}	6.46×10^{-4}	3.60	3.22

4. Example

Obtained resistance model is now used in a simple example of reliability assessment of a building structure, regarding safety (Matos *et al*. 2012). In this case, the resistance model is given by the failure load model, F_R, whose parameters are provided at Table 12 for both beams. In order to compare resistance and loading curves it is necessary to transform the obtained resistance model into a model for maximum bending moment at middle span, M_R, being the beam span, L, in this situation, equal to 4.50 m. Then, it is necessary to determine the loading curve, according to JCSS (2001). In order to do that it is required to determine the influence length of the analyzed beam, L_{inf}, which is, in this example, of 4.00 m. The applied load, p, is the sum of self-weight and live-loads multiplied by the beam influence length. It is then possible to compute the maximum bending moment, M_S.

Obtained values are then adjusted to a Normal PDF. In order to compare resistance and loading curves a limit state function, Z, is defined. This limit state is exceeded when loading is higher than resistance, Eq. (9)

$$\begin{cases} M_R = (F_R \cdot 2)/2 \cdot (L/2 - L_F) \\ M_S = (p \cdot L^2)/8 \end{cases} \Rightarrow Z = M_R - M_S \tag{9}$$

The further steps consist in computing the failure probability. On Table 13 are represented both failure probabilities and reliability indexes for all models, considering Beam 1 and 2.

In this example, the building is of class 2 (apartment building – risk to life, given a failure, is medium or economic consequences are considerable) and of class B (normal cost of safety measure), according to JCSS (2001). Therefore, a target reliability index, β_{target}, of 3.30 is recommended.

The following conclusions are then obtained for Beam 1: (1) when considering the initial values or those from model identification in service phase the beam is classified as unsafe; (2) when the values from model identification until failure are taken into account, the beam is considered to be safe; (3) obtained results for all models, considering a Bayesian inference approach, indicate that the beam is classified as safe. This means that the probabilistic-based assessment revealed an additional strength capacity which was not accounted in design. Regarding Beam 2 it is possible to verify that all evaluated models are considered to be unsafe.

5. Conclusions

A cutting-edge methodology for probabilistic-based assessment of existing structures is presented in this paper. The developed algorithm consists in two main steps: (1) model identification, in which the numerical model is updated until an established stopping criterion is met; (2) reliability assessment, in which the updated deterministic model, coming from the model identification step, is converted into a probabilistic model, being then executed the probabilistic module. Within the probabilistic module, each parameter PDF could be updated through a built-in Bayesian inference procedure, based on complementary gathered data.

The probabilistic assessment of two composite beams which were loaded at laboratory up to failure is then presented. The first beam presents a full shear connection, while the other is partially connected. All other properties are maintained. Consequently, while the former presents a typical failure mode of bending with concrete crushing and yielding of steel profile, the latter presents a combined failure mode of bending and shear connection.

In this analysis, a nonlinear numerical model was developed. A sensitivity analysis is further executed to identify the most important parameters. Some of them were characterized with detail at laboratory. The developed numerical model is then adjusted to experimental data, through a model identification procedure. To perform that, an optimization technique, based in the evolutionary strategies algorithm in its plus version, was used. Both modelling and measurement errors were considered in the algorithm stopping criteria. This procedure was developed for both service region and up to failure.

Further, a nonlinear probabilistic analysis was executed. In order to do so, a PDF is respectively assigned to each critical parameter. Such parameters are then updated with complementary data from laboratory characterization tests, through a Bayesian inference approach. From the probabilistic analysis it was obtained an updated resistance PDF for both analyzed beams. These models are then used in a safety assessment example.

The following conclusions were obtained from the probabilistic-based assessment of composite steel-concrete beams: (1) model identification up to failure load gives very good results (errors less than 10%); (2) obtained values from model identification confirmed that used materials quality is closer, or slightly higher, to the initial estimates; (3) model identification in service phase only gives good results in service region, being the obtained results in failure region unsatisfactory; (4) complementary tests, such as non-destructive tests or permanent monitoring systems, are thus recommended when performing model identification in service phase; (4) Bayesian inference increases the accuracy of the probabilistic models; (6) an additional strength capacity is identified.

The structural behavior of composite steel-concrete structures is complex, with high uncertainty, being hard to predict. Thus, it is verified that, by collecting information regarding some model parameters and by applying the developed framework, it is possible to forecast its behavior with a higher accuracy. Moreover, the fitness function allows to incorporate several measurement sources at the same time, making the model identification more robust and efficient, particularly, when studying the interface, whether in service or failure region, which behavior is extremely hard to quantify and predict. Accordingly, with this framework it will be possible to assess the structural behavior through a more robust and accurate way, being also possible to quantify any additional strength capacity. Therefore, the obtained results pointed out a relevant improvement in reliability assessment, allowing a more fundamental decision regarding the repair and strengthening of existing composite steel-concrete structures.

References

Barbato, M., Zona, A. and Conte, J. (2014), "Probabilistic nonlinear response analysis of steel-concrete composite beams", *J. Struct. Eng.*, **140**(1), 04013034.

Bergmeister, K., Novák, D., Pukl, R. and Cervenka, V. (2009), "Structural assessment and reliability analysis for existing engineering structures, theoretical background", *Struct. Infra. Eng.*, **5**(4), 267-275.

Bernardo, J.M. and Smith, A.F.M. (2004), *Bayesian Theory*, John Wiley & Sons, Ltd., Chichestc, England, Chichestc, England.

Beyer, H.-G. and Schwefel, H.-P. (2002), "Evolution strategies – A comprehensive introduction", *Natural Comput.*, **1**(1), 3-52.

Casas, J.R. and Wisniewski, D. (2011), "Safety requirements and probabilistic models of resistance in the assessment of existing railway bridges", *Struct. Infra. Eng.*, **9**(6), 529-545.

Caspeele, R. and Taerwe, L. (2014), "Influence of concrete strength estimation on the structural safety assessment of existing structures", *Construct. Build. Mater.*, **62**, 77-84.

Červenka, V., Jendele, L. and Cervenka, J. (2009), *ATENA® Program Documentation*, *Part 1: Theory*, Prague, Czech Republic.

EN 1992-1-1 (2004), Eurocode 2: Design of concrete structures - Part 1-1: General rules and rules for buildings,;European Committee for Standardization (CEN), Brussels, Belgium.

EN 1993-1-1 (2010), Eurocode 3: Design of steel structures – Part 1-1: General rules and rules for buildings; European Committee for Standardization (CEN), Brussels, Belgium.

EN 1994-1-1 (2004), Eurocode 4: Design of composite steel and concrete structures - Part 1-1: General Rules and Rules for Buildings; European Committee for Standardization CEN, Brussels, Belgium.

EN 10025-1 (2004), Hot rolled products of structural steels. Part 1: General technical delivery conditions; European Committee for Standardization (CEN), Brussels, Belgium.

EN 10025-2 (2004), European structural steel standard: Grade designations, properties and nearest equivalents; European Committee for Standardization (CEN), Brussels, Belgium.

Enright, M.P. and Frangopol, D.M. (1999), "Reliability-based condition assessment of deteriorating concrete bridges considering load redistribution", *Struct. Safety*, **21**(2), 159-195.

Enevoldsen, I. (2001), "Experience with probabilistic-based assessment of bridges", *Struct. Eng. Int.*, **11**(4), 251-260.

EuroLightCon (2000), Mechanical Properties of LWAC compared with both NWC and HSC; BE96-3942/R27, EuroLightCon - Economic Design and Construction with Lightweight Aggregate Concrete.

Goulet, J.-A., Kripakaran, P. and Smith, I.F.C. (2009), *Estimation of Modelling Errors in Structural System Identification*, Zurich, Switzerland.

Henriques, A.A.R. (1998), "Application of new safety concepts in the design of structural concrete (Aplicação de novos conceitos de segurança no dimensionamento do betão estrutural)", Ph.D. Dissertation; Universidade do Porto, Porto, Portugal. [In Portuguese]

Iman, R.L. and Conover, W.J. (1982), "A distribution-free approach to inducing rank correlation among input variables", *Commun. Statistics – Simul. Comput.*, **11**(3), 311-334.

Jacinto, L.A. (2011), "Safety assessment of existing bridges - Bayesian probabilistic approach (Avaliação da Segurança de Pontes Existentes - Abordagem Probabilística Bayesiana)", Ph.D. Dissertation; Universidade Nova de Lisboa, Lisboa, Portugal. [In Portuguese]

JCGM (2008), Evaluation of measurement data - Guide to the expression of uncertainty in measurement, JCGM 100:2008.

JCSS, J.C.o.S.S. (2001), *Probabilistic Model Code*, (12th Draft), JCSS - Joint Committee on Structural Safety.

Leming, M.L. (1988), "Properties of high strength concrete - An investigation of high strength concrete characteristics using materials in North Carolina", 23241-86-3; North Carolina State University, Raleigh, NC, USA.

Matos, J.C. (2013), *Uncertainty Evaluation of Reinforced Concrete and Composite Structures Behavior*, Ph.D. Dissertation; Escola de Engenharia, Guimarães, Portugal.

Matos, J.C., Valente, M.I.B., Neves, L.C. and Cruz, P.J.S. (2011), *Avaliação probabilística do comportamento até à rotura de estruturas: aplicação a vigas mistas*, Guimarães, Portugal.
Matos, J.C., Valente, M.I.B., Cruz, P.J.S. and Neves, L.C. (2012), *Uncertainty Evaluation of the Behavior of a Composite Beam*, Lake Maggiore–Italy.
Matos, J.C., Cruz, P.J.S., Valente, I.B., Neves, L.C. and Moreira, V.N. (2015), "An innovative framework for probabilistic-based structural assessment with an application to existing reinforced concrete structures", *Eng. Struct.*, **111**, 552-564.
Mujagić, J.R.U. and Easterling, W.S. (2009), "Reliability assessment of composite beams", *J. Construct. Steel Res.*, **65**(12), 2111-2128.
Nowak, A.S., Szersen, M.M., Szeliga, E.K., Szwed, A. and Podhorecki, P.J. (2008), "Reliability-based calibration for structural concrete, Phase 3", PCA R&D Serial No. 2849; Portland Cement Association.
Olsson, A., Sandberg, G. and Dahlblom, O. (2003), "On Latin hypercube sampling for structural reliability analysis", *Structural Safety*. **25**(1), 47-68.
Roik, E.H.K., Hanswille, G. and Lanna, A.C.-O. (1989), "Report on Eurocode 4. Clause 6.3.2.: Stud Connectors, Harmonisation of the European Construction Codes, Eurocode 3, 4 and 8 / part 3", EC4/8/88, Institut für Konstruktiven Ingenieurbau.
Rücker, W., Hille, F. and Rohrmann, R. (2006), "F08a - Guideline for the Assessment of Existing Structures", Federal Institute of Materials Research and Testing (BAM).
Shields, M.D., Teferra, K., Hapij, A. and Daddazio, R.P. (2015), "Refined Stratified Sampling for efficient Monte Carlo based uncertainty quantification", *Reliability Engineering & System Safety*. **142**,310-325.
Strauss, A., Frangopol, D.M. and Kim, S. (2008), "Use of monitoring extreme data for the performance prediction of structures: Bayesian updating", *Eng. Struct.*, **30**(12), 3654-3666.
Valente, I.B. (2007), *Experimental studies on shear connection systems in steel and lightweight concrete composite bridges*, Ph.D. Dissertation, University of Minho, Guimarães, Portugal.
Valente, I.B. and Cruz, P.J. (2010), "Experimental analysis on steel and lightweight concrete composite beams", *Steel and Composite Structures*. **10**(2), 169-185.
Valum, R. and Nilsskog, J.E. (1999), *Production and Quality Control of High Performance Lightweight Concrete for the Raftsundet Bridge*, Sandefjord, Norway.
Zona, A., Barbato, M. and Conte, J.P. (2006), "Finite element response sensitivity analysis of continuous steel-concrete composite girders", *Steel Compos. Struct., Int. J.*, **6**(3), 183-202.
Zona, A., Barbato, M., Dall'Asta, A. and Dezi, L. (2010), "Probabilistic analysis for design assessment of continuous steel–concrete composite girders", *J. Construct. Steel Res.*, **66**(7), 897-905.

CC